Journal of Visualization, Vol. 7, No. 2 (2004) 143-150

3D Visualization of the Separated Fluid Flows

Gushchin, V. A.,* Kostomarov, A. V.* and Matyushin, P. V.*

* Institute for Computer Aided Design Russian Academy of Sciences (ICAD RAS)
19/18, 2nd Brestskaya str., 123056 Moscow, Russia.

Received 1 August 2002
Revised 15 October 2003

Abstract : For the detailed investigation of the 3D unsteady incompressible viscous separated fluid flows around a sphere (for $200 \leq Re \leq 700$) and a circular cylinder (for $200 \leq Re \leq 400$) the direct numerical simulation and 3D visualization are used. For 3D visualization of the fluid flows around a sphere the definition of vortex core as a connected region containing two negative eigenvalues of the $\mathbf{S}^2+\mathbf{\Omega}^2$ tensor is used (where $\mathbf{S}_{i,j}$ and $\mathbf{\Omega}_{i,j}$ are the rate of strain and the rate of rotation tensors). The formation mechanism of vortices in the sphere wake for Re=500 is described in detail. For 3D visualization of the fluid flows around a circular cylinder the 3D isosurfaces of the streamwise component of vorticity ω_x are used.

Keywords : 3D Visualization, Sphere, Cylinder, Wake, Vortex structures

1. Introduction

The understanding of the dynamics and kinematics of the 3D unsteady separated fluid flows around the bluff bodies is very important both from theoretical and from practical point of view. With the development of high-performance computers and especially cost effective massive parallel computers with a distributed memory the numerical simulation becomes one of the more effective approaches for such investigations. The 3D velocity and pressure fields calculated by this numerical simulation can not explain us the dynamics and kinematics of the 3D unsteady separated fluid flows without the appropriate 3D visualization of them.

Detailed investigations of the structure of the sphere wake in the homogeneous fluid have been initiated in (Magarvey and Bishop, 1961) and prolongated in (Sakamoto and Haniu, 1990, 1995), (Gushchin and Matyushin, 1997), (Johnson and Patel, 1999), (Gushchin et al., 1998, 2001, 2002) and other papers. In spite of these papers, the detailed formation mechanism of vortices in the sphere wake is still unclear.

In the present work the direct numerical simulation is used for the detailed investigation of transitional (from 2D to 3D unsteady) and post transitional regimes of 3D separated incompressible viscous fluid flows around a sphere and a 3D circular cylinder. The governing Navier-Stokes equations are written as follows:

$$\frac{\partial \vec{\mathbf{v}}}{\partial t} + (\vec{\mathbf{v}} \bullet \nabla)\vec{\mathbf{v}} = -\nabla p + \frac{2}{Re}\Delta \vec{\mathbf{v}} \tag{1}$$

$$\nabla \bullet \vec{\mathbf{v}} = 0 \tag{2}$$

where $\vec{\mathbf{v}}$ is velocity vector (non-dimensionalized by the uniform velocity U), p – pressure (non-dimensionalized by the ρU^2, where ρ is fluid density (ρ=1)), $Re = Ud/\nu$ is Reynolds number, d is diameter of a sphere, ν is the coefficient of kinematic viscosity, distances are non-dimensionalized by the radius of the sphere $d/2$, time is non-dimensionalized by the $d/(2\ U)$. The boundary conditions imposed on $\vec{\mathbf{v}}$ are as follows: $\vec{\mathbf{v}}$=0 on the sphere; $\vec{\mathbf{v}}$=(0,0,1) on the outer boundary.

For this direct numerical simulation the Splitting on physical factors Method for Incompressible Fluid flows (SMIF) with hybrid explicit finite difference scheme (second order of accuracy in space, minimum scheme viscosity and dispersion, capable for work in wide range of Reynolds numbers and monotonous) based on Modified Central Difference Scheme (MCDS) and Modified Upwind Difference Scheme (MUDS) with special switch condition depending on velocity sign and sign of the first and the second differences of transferred functions was developed and successfully applied (Gushchin and Konshin, 1992), (Gushchin and Matyushin, 1997). Some applications of SMIF for solving of different problems are described in (Belotserkovskii, 1997). The Poisson equation for the pressure was solved by the Preconditioned Conjugate Gradients Method. Each time step was chosen automatically from a scheme stability condition. The parallelization of the algorithm was made and successfully applied on massive parallel computers with a distributed memory such as PARAM 10000 (based on Ultra Sparc II processors (400 MHz)) and MBC 1000/17IAP (based on the Intel Xeon processors (1.7 GHz)).

In order to understand the dynamics and kinematics of the 3D unsteady separated fluid flows we must properly visualize the 3D vortex structures of the wake. We need more than the 2D visualization of streamlines, pressure contours (isolines), vorticity contours in the some planes. In many cases the 3D isosurfaces of pressure or of vorticity can not also give us the real vortex structures of the wake. A number of methods have been proposed for properly identifying vortical regions. Jeong and Hussain(1995) have reviewed these methods and have proposed a new method They identified the vortical regions by using the definition of vortex core as a connected region containing two negative eigenvalues of the $\mathbf{S}^2+\mathbf{\Omega}^2$ tensor (where the rate of strain $\mathbf{S}_{i,j}$ and rate of rotation $\mathbf{\Omega}_{i,j}$ tensors are $\mathbf{S}_{i,j}=(v_{i,j}+v_{j,i})/2$, $\mathbf{\Omega}_{i,j}=(v_{i,j}-v_{j,i})/2$). Jeong and Hussain provide number of examples to illustrate the advantages of this method over others, indicating a more robust and precise elucidation of the vortex regions. We are successfully applied this method for our 3D flow visualization (see Fig. 1 (a), where one quadrant of the vortex structure was cut away in order to see the sphere surface (blue color)).

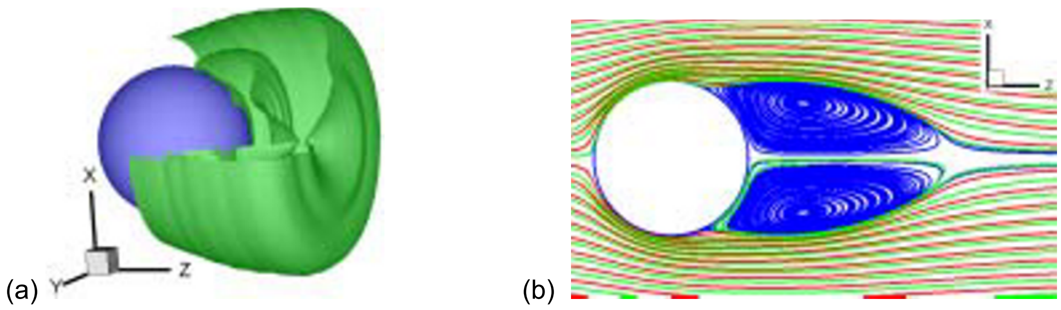

Fig. 1. Re=200: (a) Vortex Structure (Zero Isosurface of the Second Eigenvalues of the $\mathbf{S}^2+\Omega^2$ Tensor) ; (b) Streamlines in the Symmetry Plane of the Wake.

2. 3D Visualization of the Flow around a Sphere

For the investigation of the 3D unsteady separated homogeneous viscous fluid flows around the sphere the spherical coordinate system (O-type grid) is used: $x = R\sin\theta\cos\varphi$, $y = R\sin\theta\sin\varphi$, $z = R\cos\theta$, where z, x, y are streamwise, lift and lateral directions, accordingly (see Fig. 1 (a)). For appropriate approximation of the boundary layer the following transforming function in radius direction was used:

$$R_i = R(r_i) = 1 + \frac{i}{N_0}\sqrt{\frac{2}{\mathrm{Re}}} + \left(\frac{i}{N} r_{\max}\right)^m \quad i=1{:}N \qquad m=3,\ r_{\max}=3,\ N=120,\ N_0=10 \tag{3}$$

where N_0 is the number of grid points in the boundary layer in radial direction. The following number of grid points (r, θ, φ) is used: (120 x 60 x 120). Methodical calculations for checking the grid dependency was carry out in (Matyushin, 2003) where was shown that for $Re \le 500$ the reasonable grid independence is achieved on a (120 x 60 x 120) grid with $N_0 = 10$.

At the present paper the classification of the 3D separated homogeneous viscous fluid flow regimes around the sphere at $0 \le Re \le 700$ was refined. For $0 \le Re \le 20.5$ the streamlines follow the sphere surface without separation. For $20.5 \le Re \le 270$ the separated fluid flows around a sphere are steady. For $20.5 \le Re \le 200$ the axisymmetrical separated fluid flows around a sphere were observed (see Fig. 1). The vortex structure in Fig. 1 (a) is divided into the recirculating zone of the wake (which is clearly seen in Fig. 1 (b) also) and a cylindrical separated shear layer (vortex sheet) at the periphery of the recirculating zone (which is invisible in Fig. 1 (b)). For $200 < Re \le 270$ the main axisymmetrical bubble (toroid) in the recirculating zone of the wake and cylindrical shear layer are deformed through a normal bifurcation in more topologically stable form (a double-thread wake (Fig. 2)). The 3D particle path (streamline) in Fig. 2 (b) reveals that there is a fluid which is flowing out from the centre of the upper part of the vortex in the recirculating zone of the wake and feeding into the centre of the lower part of this vortex through the core of the deformed toroid. Moreover the lower spiral (unstable focus) which is fed by fluid from the upper spiral (stable focus) releases fluid into the wake after sending it up and around the toroid. (In stable focus the liquid moves along a spiral towards its centre; in unstable focus the liquid moves along a spiral outwards its centre (Tobak and Peake, 1982).) In the Fig. 2 (b) you can see also skin friction patterns on the sphere surface which reveal primary separation line with two singular points (node and saddle) and rear stagnation point. The steady flows for $200 < Re \le 270$ are characterised by the existence of non-zero lift/side and torque moment coefficients (see (Magarvey and Bishop, 1961), (Johnson and Patel, 1999), (Gushchin et al., 1998, 2001, 2002)).

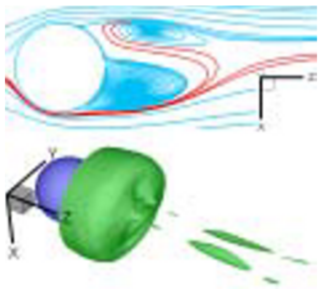
(a)

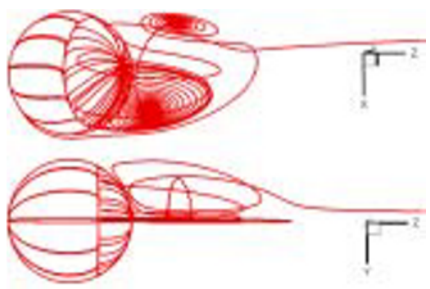
(b)

Fig. 2. Re=211: (a) (top) Streamlines in the Symmetry Plane of the Wake.
(a) (bottom) Vortex Structure. (Zero Isosurface of the Second Eigenvalues of the $\mathbf{S}^2+\Omega^2$ Tensor)
(b) 3D Streamline and Skin Friction Patterns on the Sphere Surface: oblique and Y-Z Views

For $Re > 270$ the wake becomes unsteady through a Hopf bifurcation and the separated fluid flows around a sphere are unsteady and periodical. For $270 < Re < 400$ periodical separation of the hairpin-shaped vortices is observed only from one (top) edge of cylindrical shear layer surrounding the recirculating zone (see Fig. 3), and the time-averaged lift/side and torque moment coefficients are not equal to zero. Besides for $360 \le Re < 400$ the regular rotation of the wake is observed (Strouhal numbers corresponding to this rotation are $St_{\mathrm{rot}} = 0.0044$, 0.0058 for $Re = 375$, 380 accordingly). ($St_{\mathrm{rot}} = f_{\mathrm{rot}} d/U$, where f_{rot} is the rotation frequency.) The Strouhal number for $Re = 300$ is St=0.145 ($St = fd/U$, where f is the shedding frequency). For the same $Re = 300$ the experimental results (Sakamoto and Haniu, 1990) give a Strouhal number range of 0.150-0.165 and the numerical result (Johnson and Patel, 1999) gives the value of 0.137 for Strouhal number. The vortex structure visualization in (Johnson and Patel, 1999) is very close to Fig. 3. Note that in Fig. 3 the vortex structures show not only the hairpin vortices separated from the top of the sphere and facing upwards, but also additional vortices (facing downwards) induced by the interaction of the near wake flow and the outer flow.

For $Re \geq 400$ the periodical separation of the hairpin-shaped vortices is observed from opposite edges of the cylindrical shear layer alternatively and the time-averaged lift/side coefficients of such flows are equal to zero (see Figs. 4-7). For $Re > 600$ the irregular rotation of the cylindrical shear layer, is observed.

The Strouhal numbers (see Table 1) obtained in this work are in a good agreement with experiment (Sakamoto and Haniu, 1990) ($0.15 < St < 0.2$) and other experimental and numerical results.

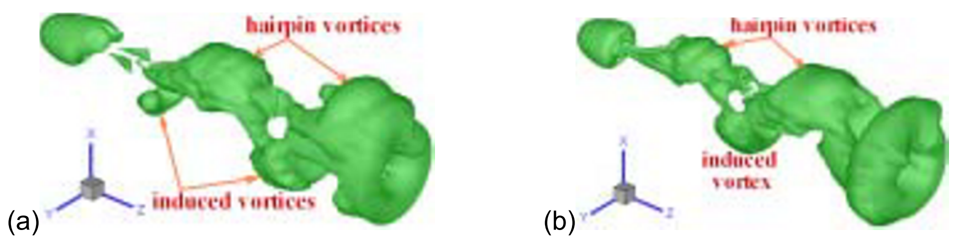

Fig. 3. *Re*=300 : Vortical Structures: (a) *t*=775, (b) *t*=782.
(Zero Isosurfaces of the Second Eigenvalues of the $\mathbf{S}^2+\Omega^2$ Tensor)

Table 1. Strouhal Numbers *St*, Time-averaged Lateral C_l and Drag C_d Coefficients versus *Re.*

Re	280	290	300	350	360	375	380	390	400	500	600	700
St	0.133	0.140	0.145	0.141	0.160	0.191	0.193	0.154	0.135	0.112	0.142	0.150
C_l	0.078	0.082	0.084	0.086	0.084	0.082	0.083	0.081	0.0	0.0	0.0	0.0
C_d	0.683	0.675	0.669	0.636	0.630	0.622	0.619	0.615	0.607	0.582	0.561	0.536

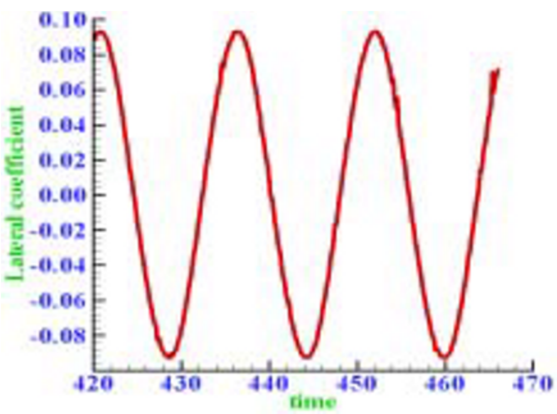

Fig. 4. *Re*=500: The total Lateral Coefficient Versus Time.

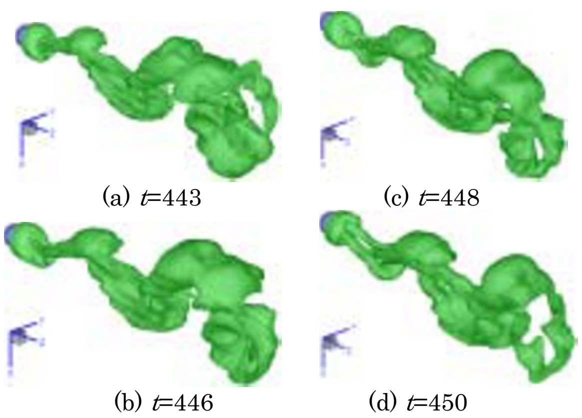

Fig. 5. *Re*=500: Vortex Structures during a Half of the Period: $443<t<450$.(Zero Isosurfaces of the Second Eigenvalues of the $\mathbf{S}^2+\Omega^2$ Tensor)

The detail formation mechanism of vortices in the sphere wake for $Re \geq 400$ is shown in Figs. 5-7 where the separation of the hairpin-shaped vortex from bottom edge of the cylindrical shear layer (vortex sheet) during a half of the period ($443 < t < 450$) is observed at $Re = 500$. (Dimensionless time step dt is equal to 0.0002.) In Fig. 6 the more detail views of the vortex structures from Fig. 5 are presented (one half of the vortex structure is removed for clarity). This formation mechanism can be divided in four stages. In Fig. 6 (a) (at the first stage) you can see the recirculating zone (in the vicinity of the sphere surface), the cylindrical shear layer (at the periphery of the recirculating zone) and the deformed vortex loop (facing upwards). The lower part of this deformed vortex loop belongs to the lower part of the recirculating zone. Unlike flow regimes for $Re < 400$ for this flow regime there is no deformed vortex ring in the recirculating zone (see Fig. 6). Therefore the upper and lower foci in Fig. 7 belong to the different vortex structures. The lower and upper foci in Figs. 6 (a) and 7 (a) belong to the lower and upper parts of the recirculating zone correspondingly.

At the second stage the bottom part of the deformed vortex loop (facing upwards) is extracted from the lower part of the recirculating zone (which is shifted closer to the sphere) and the bottom and side parts of the vortex sheet grow and undergo a stretching process (see Fig. 6 (b)). At the third stage the bottom edge of the vortex sheet is rolling up cylindrically and detached from the vortex sheet; the lower part of the recirculating zone is connected with the bottom part of the vortex sheet; the top and side parts of the deformed vortex loop are separated as hairpin-shaped vortex loop (facing upwards) (Fig. 6 (c)). At the fourth stage the bottom and side edges of the vortex sheet are transformed into the front and side parts of the nascent deformed vortex loop (facing downwards) (see Fig. 6 (d)).

During the next half of the period the front and side parts of the nascent deformed vortex loop (facing downwards) (see Fig. 6 (d)) are separated as hairpin-shaped vortex loop (facing downwards); the top and side edges of the vortex sheet are transformed into the front and side parts of the next nascent deformed vortex loop (facing upwards) and so on.

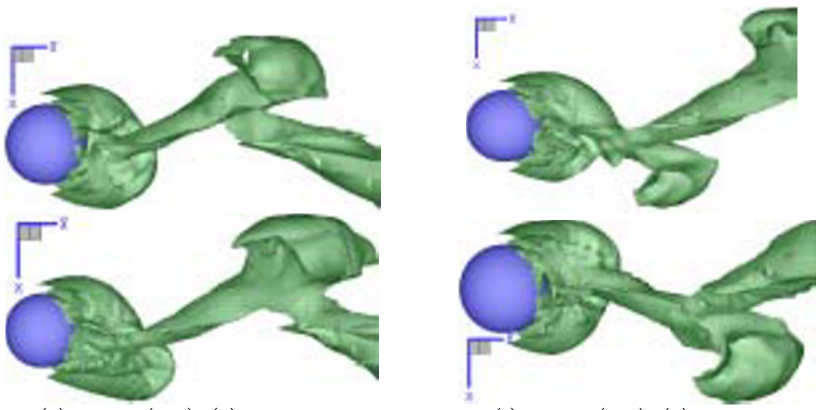

(a) t=443 (top), (b) t=446 (c) t=448 (top), (d) t=450

Fig. 6. Re=500: Vortex Structures during a Half of the Period: $443 < t < 450$.(Zero Isosurfaces of the Second Eigenvalues of the $\mathbf{S}^2+\Omega^2$ Tensor).

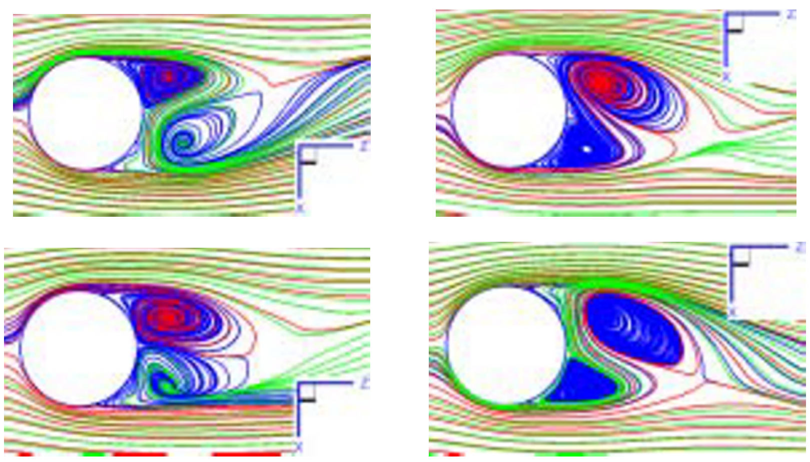

(a) t=443 (top), (b) t=446 (c) t=448 (top), (d) t=450

Fig. 7. Re=500: Streamlines in Symmetry Plane of the Wake: $443 < t < 450$.

3. The Visualization of the Vortex Structures in the Wake of a 3D Circular Cylinder

The transitional regimes of the separated homogeneous fluid flows around a 3D circular cylinder have been investigated in (König and Eckelmann, 1995), (Williamson, 1996), (Braza, 1998) and other papers. It was determined that flow in the wake of the 3D circular cylinder became 3D for $Re > 191$. In this paper transitional regimes of the separated homogeneous fluid flows around a 3D circular cylinder were investigated for $200 \le Re \le 400$. For this investigation the cylindrical coordinate system (O-type grid) is used: $x = R\cos\theta,\ y = R\sin\theta,\ z = z$, where x, y, z are streamwise, lift and spanwize directions, accordingly. From the methodical calculations for 2D circular cylinder (see (Gushchin et al., 2002)) the following conclusions were made: for moderate Reynolds numbers ($100 \le Re \le 400$) the grid in radial and circumferential directions should be at least 180 x 180 or 240 x 240, the number of the points in the boundary layer can be taken not less than 5, the location of the outer boundary $23.78d$ with usual ($\vec{\mathbf{v}}$=(1,0,0)) or non-reflecting boundary conditions is sufficient to see the effects in the near wake region ($0.5d < x < 10d$) (d is the diameter of the cylinder). The set of the 3D calculations for the optimal flow parameters (grid size (r, θ, z) - 240x240x72, 10 points in the boundary layer, location of the outer boundary - $23.78d$, the length of the cylinder - L=$7.5d$) was executed for Re=220, 240, 260, 280, 300, 320, 340, 360, 400. In addition the 3D calculations for the different length of the cylinder ($3.5d < L < 15d$) and different Re numbers ($200 \le Re \le 400$) were performed. Some examples of these combinations (L, Re) are listed bellow: ($3.5d$, 250), ($4.4d$, 400), ($7d$, 230), ($11.5d$, 230).

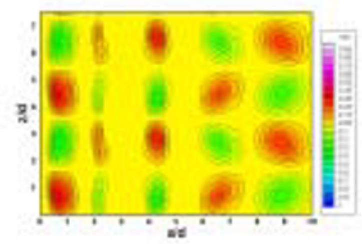

Fig. 8. Isolines of the Streamwise Component of Vorticity ω_x in the Plane $y = 0$
Mode A, Re = 220, L=7.5d.

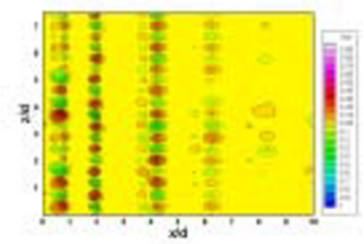

Fig. 9. Isolines of the Streamwise Component of Vorticity ω_x in the Plane $y = 0$
Mode B, Re = 320, L=7.5d.

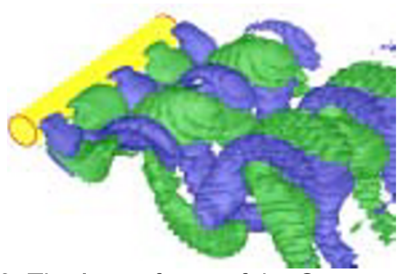

Fig. 10. The Isosurfaces of the Streamwise Component of Vorticity ω_x
Mode A, Re = 240, L=7.5d.

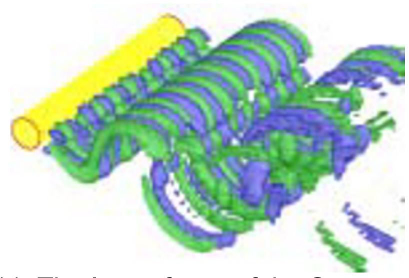

Fig. 11. The Isosurfaces of the Streamwise Component of Vorticity ω_x
Mode B, Re = 320, L=7.5d.

We observe the mode A for $191 \le Re \le 300$ and mode B for $300 \le Re \le 400$. The isolines of the streamwise component of vorticity ω_x in the plane $y = 0$ for modes A and B are shown in the Figs. 8 and 9 correspondingly ($\vec{\boldsymbol{\omega}} = rot\ \vec{\mathbf{v}}$). In these figures the negative values of ω_x are green, the positive values are red. From these figures the periodicity along z axis is easily seen. For mode A and B the periods along z axis are equal to $3.5d \le \lambda \le 4d$ and $0.8d \le \lambda \le 1.0d$ correspondingly. It is worth noting that vortex structures for mode A, obtained for different Re numbers coincide qualitatively and distinguish by the intensity of vortex only. (Same for mode B).

The isosurfaces of the streamwise component of vorticity ω_x are shown in Figs. 10 and 11. Similar visualization was used in works (Williamson, 1996), (Braza, 1998). In this work for the first time the values of the maximum phase difference along the span were estimated. These values are approximately equal to 0.1-0.2 T(for mode A) and 0.015-0.030 T(for mode B), where T is the period of the flow. For Re = 300 obtained both modes A and B are existing simultaneously.

In Figs. 12 and 13 the negative and positive values of the spanwise component of vorticity ω_z are visualized on the rear part of the surface of the cylinder (the θ–coordinate starts from front stagnation line). The negative values of ω_z are blue, the positive values of ω_z are red. The separation and adhesion of the flow from the surface of the cylinder occurs on the lines with zero ω_z.

In the Figs. 14 and 15 the streamlines in the x–y planes for $z = 0.73d$ and $z = 2.6d$ are visualized at the same time. These pictures demonstrate the phase difference along the span of the cylinder. In Fig. 14 the joined vortex in the upper plane is already developed, but in the Fig. 15 the joined vortex in the upper plane is not developed yet.

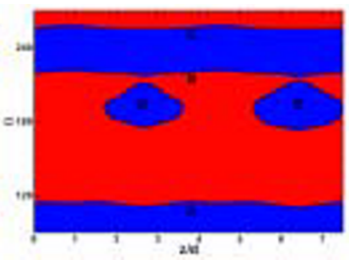

Fig. 12. The Spanwize Component of Vorticity ω_z on the Surface of the Cylinder. Red are the Positive Values, Blue are the Negative Values. Mode A. Re = 220, L=7.5d.

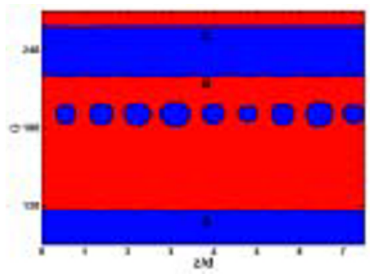

Fig. 13. The Spanwize Component of Vorticity ω_z on the Surface of the Cylinder. Red are the Positive Values, Blue are the Negative Values. Mode B. Re = 320, L=7.5d.

Fig. 14. The Streamlines in the Plane Z=0.73d, Re=260, L=7.5d.

Fig. 15. The Streamlines in the Plane Z=2.6d, Re=260, L=7.5d.

4. Conclusion

The numerical method SMIF successfully applied in the present work showed a good comparison of our results with experimental and numerical works of the other researchers. The 3D visualization developed and used here gave us a possibility for more careful analysis of the transitional flow regimes around the sphere and the 3D circular cylinder and the further understanding and refining of classification of these flow regimes. For the first time in this paper the formation mechanism of vortices in the sphere wake for $Re \geq 400$ was described in detail and the values of the maximum phase difference along the span of 3D circular cylinder was estimated for modes A and B.

This work is supported by Russian Foundation for Basic Research (grants № 02-01-00557 and № 03-01-06325); by the program “Mathematical Modeling” of the Presidium of the Russian Academy of Sciences; by the grant of the President of Russian Federation for support of the leading scientific schools № SS-70.2003.1 and by the program for Basic Research № 3 of the Department of the Mathematical Science of the Russian Academy of Sciences.

References

Belotserkovskii, O. M., Mathematical modelling in Informatics: Numerical Simulation in the Mechanics of Continuous Media, Moscow State University of Printing Arts, Moscow, Russia.(1997)

Braza, M., The 3D Transition to Turbulence in Wake Flows by Means of Direct Numerical Simulation, J. Flow Turbulence and Combustion, 63 (1999), 315-341.

Gushchin, V. A. and Konshin, V. N., Computational Aspects of the Splitting Method for Incompressible Flow with a Free Surface, Journal of Computers and Fluids, 21-3 (1992), 345-353.

Gushchin, V. A., Kostomarov, A. V., Matyushin, P. V. and Pavlyukova, H. R., Numerical Investigation of 3D Separated Fluid Flows Around a Sphere, Proceedings of the Third Asian Computational Fluid Dynamics Conference , Editors: T. S. Prahlad, S. M. Deshpande, S. K. Saxena, (Bangabe, India),2 (1998-12), 231-236.

Gushchin, V. A., Kostomarov, A. V., Matyushin, P. V. and Pavlyukova E. R., Direct Numerical Simulation of the Transitional Separated Fluid Flows around a Sphere, Japan Society of CFD/CFD Journal, 10-3 (2001), 344-349.

Gushchin, V. A. Kostomarov, A. V., Matyushin, P. V. and Pavlyukova, E. R., Direct Numerical Simulation of the Transitional Separated Fluid Flows Around a Sphere and a Circular Cylinder, Journal of Wind Engineering & Industrial Aerodynamics, 90/4-5 (2002), 341-358.

Gushchin, V. A. and Matyushin, P. V. Numerical Simulation of Separated Flow Past a Sphere, Computational Mathematics and Mathematical Physics, 37-9 (1997), 1086-1100.

Jeong, J. and Hussain, F., On the Identification of a Vortex, J. Fluid Mech., 285 (1995), 69-94.

Johnson, T. A. and Patel, V. C., Flow Past a Sphere up to a Reynolds Number of 300, J. Fluid Mech., 378 (1999), 19-70.

König, M. and Eckelmann, H., On the Transition of the Cylinder Wake, J. Phys. Fluids, 7-4 (1995),779-794.

Magarvey, R. H. and Bishop, R. L., Transition Ranges for Three-dimensional Wakes, Can. J. Phys., 39 (1961), 1418-1422.

Matyushin, P. V., Numerical Simulation of 3D Separated Homogeneous Incompressible Viscous Fluid Flows around a Sphere, Ph. D. Thesis, Institute for Computer Aided Design RAS (2003) (in Russian)

Tobak, M. and Peake, D. J., Topology of Three-dimensional Separated Flows, Ann. Rev. Fluid Mech., 14 (1982), 61-85.

Sakamoto, H., and Haniu, H., A Study of Vortex Shedding from Spheres in a Uniform Flow, Trans. ASME: J. Fluids Engng., 112 (1990), 386-392.

Sakamoto, H. and Haniu, H., The Formation Mechanism and Shedding Frequency of Vortices from a Sphere in Uniform Shear Flow, J. Fluid Mech., 287 (1995), 151-171.

Williamson, C. H. K., Three-dimensional Wake Transition, J. Fluid Mech., 328 (1996), 345-407.

Author Profile

Valentin Gushchin: He received his MSc degree in Computer Research and Applied Mathematics in 1971 from the Moscow Institute of Physics and Technology (MIPT) (Faculty of Management and Applied Mathematics); his Ph. D. (Candidate of Science degree) in Computation Mathematics in 1975 from MIPT; and his Doctor of Science degree in Application of Mathematical Modeling in science & technology in 1990 from MIPT. From 1974 he works in MIPT (Chair of Mathematics), his current position in MIPT is a full professor (mathematical analysis, analytical geometry, differential equations, The theory of probability, The theory of functions of complex variables, Equations of mathematical physics). From 1974 till 1987 he worked in the Computing Center Russian Academy of Science (CC RAS) in Moscow. From 1987 he works in the Institute for Computer Aided Design Russian Academy of Science (ICAD RAS) in Moscow. His current position is a Deputy Director of ICAD RAS, Head of Department (research and development in the field of mathematical models, numerical methods for incompressible fluid flows, investigation of separated fluid flows; development of applied package (clean rooms, heating, ventilation and aeroconditioning); parallel computing). Thus he performed more then 30 years record proven track in the mathematical modelling, parallel computing, and applied packages development for hydrodynamic problems.

Alexei Kostomarov: He received his MSc degree in Computer Research and Applied Mathematics in 1995 from Moscow Institute of Physics and Technology (Faculty of Management and Applied Mathematics). From 1995 till 1999 he was a Post graduate student in Institute for Computer Aided Design Russian Academy of Sciences (ICAD RAS) in Moscow. From 1997 he works in ICAD RAS as a scientific researcher (computations of separated incompressible viscous fluid flows around a 2D and 3D circular cylinder, simulations air, heat, and masstransfer in the Clean Rooms).

Paul Matyushin: He received his MSc degree in Computer Research and Applied Mathematics in 1993 from Moscow Institute of Physics and Technology (MIPT) (Faculty of Management and Applied Mathematics), and his Ph. D. (Candidate of Science degree) in Application of Mathematical Modeling in science & technology in 2003 from MIPT. From 1997 he works in Institute for Computer Aided Design Russian Academy of Sciences (ICAD RAS) in Moscow as a scientific researcher (investigation of 3D separated incompressible viscous fluid flows around a sphere; calculations of 2D flows around arbitrary profile).